ACS Catalysis

pubs.acs.org/acscatalysis

Research Article

Direct Synthesis of Acetone by Aerobic Propane Oxidation Promoted by Photoactive Iron(III) Chloride under Mild Conditions

Andrea Rogolino, José B. G. Filho, Lorena Fritsch, José D. Ardisson, Marcos A. R. da Silva, Gabriel Ali Atta Diab, Ingrid Fernandes Silva, Carlos André Ferreira Moraes, Moacir Rossi Forim, Matthias Bauer, Thomas D. Kühne, Markus Antonietti, and Ivo F. Teixeira*

Cite This: *ACS Catal.* 2023, 13, 8662–8669

Read Online

ACCESS | Metrics & More | Article Recommendations | Supporting Information

ABSTRACT: C−H activation of hydrocarbons is extremely challenging, especially in short-chain hydrocarbons like propane. In industry, propane is first converted to propylene mostly by steam cracking, which is only oxidized to acetone in the cumene process, yielding acetone and phenol. In this work, we show that the simple $FeCl_3$ salt in acetonitrile photocatalyzes the oxidation of propane to acetone at room temperature under aerobic conditions and visible-light irradiation. We achieved 100% conversion of propane with 67% selectivity in acetone after 4 h of irradiation and TON up to 600. Mechanistic studies, including electrospray ionization mass spectrometry, Mössbauer, and electro-paramagnetic resonance spectroscopy, concluded that the reaction is driven by chlorine radicals generated by Fe−Cl bond photolysis. These results not only hold promise for the development of solar-based oxidation of hydrocarbons but more importantly also disclose deeper insights into the largely overlooked photochemistry of $FeCl_3$.

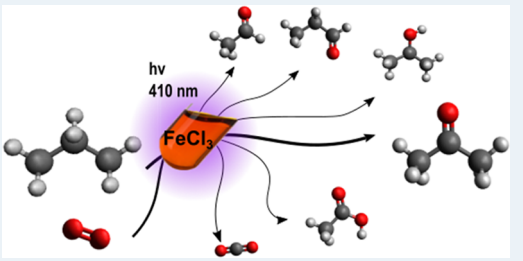

KEYWORDS: *photocatalysis, propane, iron, radical, oxidation*

INTRODUCTION

C−H activation is an energy-demanding reaction, which usually requires harsh conditions and catalysts due to the high C−H bond dissociation energies between 300 and 480 kJ mol^{-1}.[1] This is especially challenging in short-chain hydrocarbons like propane. For example, there is no industrial process capable of converting propane into acetone directly. In industry, propane is first converted to propylene mostly by steam cracking, reacted with benzene leading to cumene, which is finally oxidized, yielding acetone and phenol (cumene process).[2]

Functionalization of hydrocarbons is a fundamental chemical process to synthesize added-value chemical feedstocks from simple organic molecules generally extracted from oil. The oxidation of alkanes is one of the most important processes carried out in the petrochemical industry. Cyclohexanone and cyclohexanol, a valuable mixture for the production of adipic acid, are produced at 160 °C and 15 bar O_2 in the presence of cobalt salts.[3] Various metal complexes—including Cr,[4] Mn,[5] and Cu[6]—proved to catalyze the oxidation of alkanes in organic solvents. However, all these catalysts require high temperatures and high pressures. Conversely, Shul'pin et al.[7] verified that $FeCl_3$ could be photoactivated to promote alkane oxidations. They demonstrated that for the conversion of cyclohexane into cyclohexanone with quite modest yields (i.e. < 10%). This very simple chemistry of $FeCl_3$ seems to have been rediscovered recently. Some important examples of C−H activations photocatalyzed by $FeCl_3$ were reported in the last two years, now with significantly more attractive activities allowed by powerful LEDs as irradiation sources.[8−10]

Inspired by these works, we employed an organic solution of $FeCl_3$ to catalyze the oxidation of propane directly to acetone under visible-light irradiation in aerobic conditions. Propane was completely oxidized, yielding up to 67% of acetone in 4 h. Our detailed mechanism investigation revealed that the oxidative catalysis cannot be attributed to Fe^{IV} or Fe^{V} species. Instead, Mössbauer spectroscopy, mass spectrometry, DFT calculations, and careful catalytic tests suggested that tetracoordinated Fe^{III} bonded to chlorine and acetonitrile are the most likely active species. The reaction proceeds through the formation of chlorine radicals ($Cl^{\bullet}$) photocatalyzed by the Fe^{III} active species and subsequent hydrogen atom transfer (HAT) to generate alkyl radicals. Photocatalysis sustained by iron(III) chloride discloses a new paradigm of iron chemistry and reveals a new route to convert propane into acetone under mild conditions.

Received: May 8, 2023
Revised: June 2, 2023
Published: June 15, 2023

https://doi.org/10.1021/acscatal.3c02092
ACS Catal. 2023, 13, 8662−8669

Table 1. Catalytic Screening and Controls[a]

entry	catalyst[b]	irradiation	acid[c]	oxidant[d]	acetone (μmol)	TON
1	$FeCl_3$	410 nm	H_2SO_4	O_2	554.8	62.3
2	$FeCl_3$ $6H_2O$	410 nm	H_2SO_4	O_2	562.4	63.2
3	$FeCl_3$ $6H_2O$	none	H_2SO_4	O_2	4.8	0.5
4	$FeCl_3$ $6H_2O$	410 nm	H_2SO_4	H_2O_2	14.9	1.7
5	$FeCl_3$ $6H_2O$	410 nm	None	O_2	571.3	64.2
6	$Fe_2(SO_4)_3$ xH_2O	410 nm	H_2SO_4	O_2	7.0	0.8
7	none	410 nm	H_2SO_4	O_2	<1.0	

[a]Conditions: 2 mL CH_3CN, 2.8 bar propane (1.1 mmol), 4 h, r.t. [b]1.6 mg $FeCl_3$ or 2.4 mg $FeCl_3{\cdot}6H_2O$ or 2.1 mg $Fe_2(SO_4)_3{\cdot}xH_2O$ (8.9 μmol, 0.8 mol %). [c]5 μL H_2SO_4 98% (91.9 μmol). [d]3.4 bar O_2 or 80 μL H_2O_2 50% (1.7 mmol).

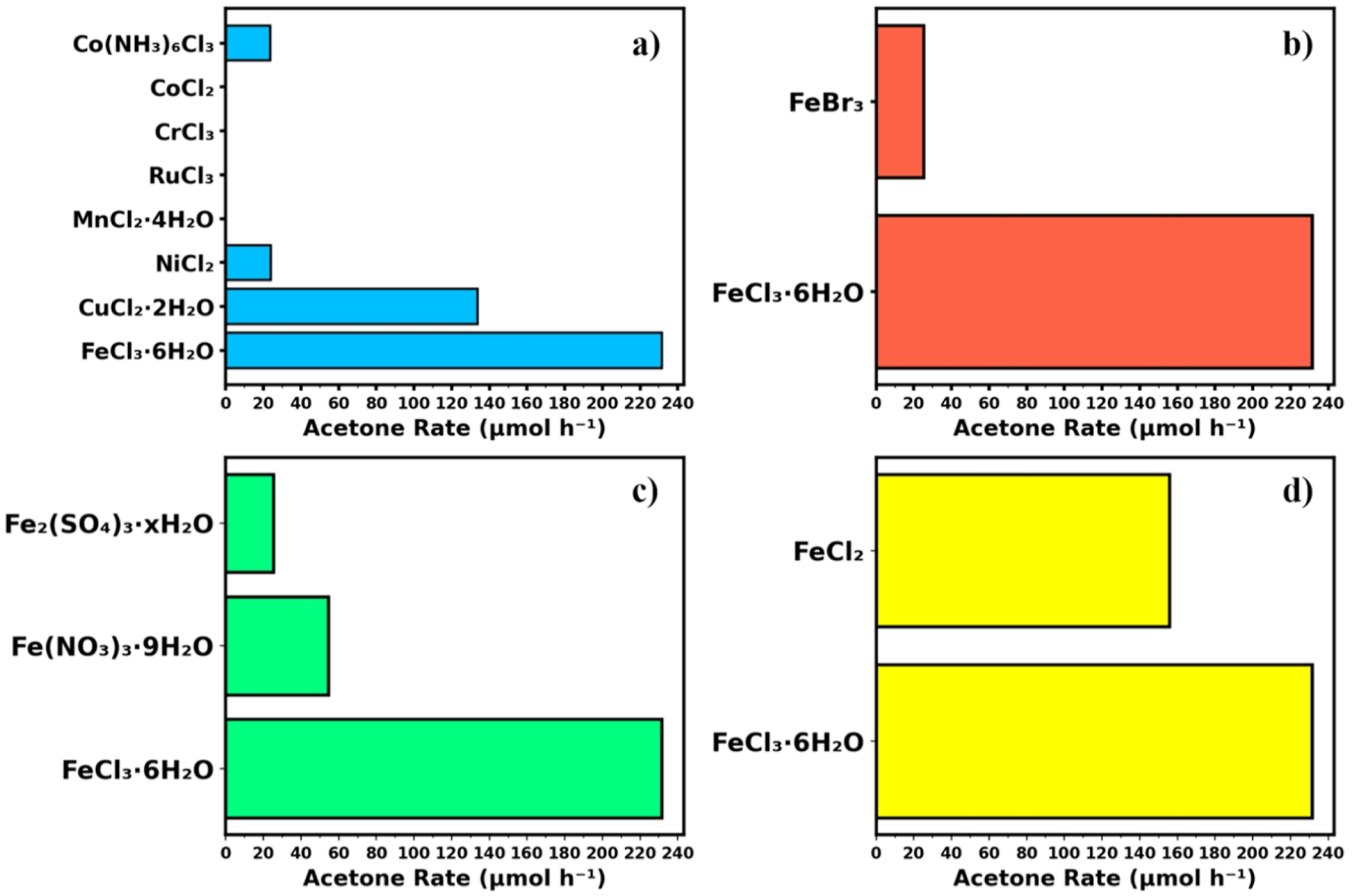

Figure 1. Catalytic screening over different variations: (a) metal chlorides, (b) iron(III) halides, (c) iron(III) salts, (d) iron oxidation state. Reaction conditions: 2 mL CH_3CN, metal salt (17.8 μmol, 1.6 mol %), 3.4 bar O_2, 2.8 bar propane (1.1 mmol), 410 nm (100 W), 1 h, r.t.

RESULTS AND DISCUSSION

Catalytic Tests and Screening. Light-assisted oxidation of propane was initially tested in an acidified solution of $FeCl_3$ in a pressurized reactor filled with gaseous propane and excess oxygen. Acetonitrile was chosen as a solvent for its inertness under oxidative conditions and suitable dissolving properties for organic substances. The reactor was irradiated in the violet region of visible light (410 nm), where iron(III) chloride in acetonitrile exhibits significant absorption (Figure S1). The absorption of visible light is also clearly demonstrated by the dark yellow color of $FeCl_3$ in acetonitrile. Acetone was initially quantified by H NMR to follow the reaction's progress. In preliminary tests, $FeCl_3$ catalyzed >50% conversion of propane to acetone in just 4 h (Table 1, entry 1). First, it was observed that anhydrous and hexahydrate forms of the salt gave no significant difference (entry 2), suggesting that the presence of water does not hamper iron(III) chloride. We then tested whether the high activity might be attributed to a general acid catalysis. However, no acetone was observed when light was turned off (entry 3); this clearly indicated the involvement of photons. When O_2 was replaced by H_2O_2, a much lower amount of acetone was recovered (entry 4). This is a strong evidence against a pure Fenton-like chemistry.[11,12] Hydrogen peroxide was thus ruled out as an intermediate in the process. Given the acidic properties of iron(III), the addition of a strong acid was considered unnecessary. When no external acid was transferred in the reactor, the photooxidation occurred slightly faster than in the presence of H_2SO_4 (entry 5). To test the effect of sulfate ions, iron(III) chloride was replaced with the sulfate analogue $Fe_2(SO_4)_3$ in equal molar amounts, and nearly no acetone was produced (entry 6), indicating that chloride ions have an important role in the reaction.

https://doi.org/10.1021/acscatal.3c02092
ACS Catal. 2023, 13, 8662−8669

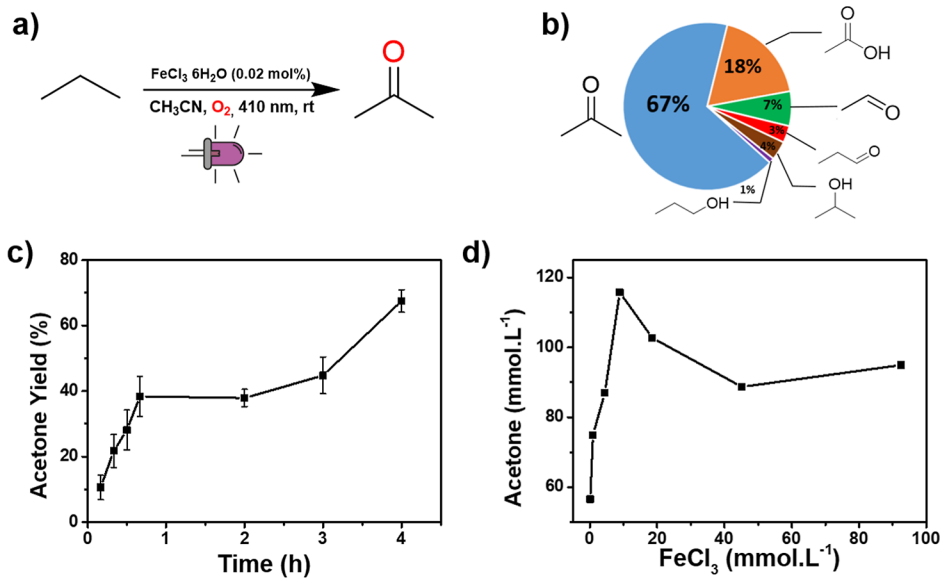

Figure 2. (a) Reaction scheme, (b) composition of the liquid phase from the best result achieved, (c) kinetics of acetone synthesis, (d) acetone synthesis as a function of $FeCl_3{\cdot}6H_2O$ concentration, Conditions: 2 mL CH_3CN, 3.4 bar O_2, 2.8 bar propane (1.1 mmol), 410 nm (100 W), r.t., (b,c) $FeCl_3{\cdot}6H_2O$ (17.8 μmol, 1.6 mol %), 1 h.

Under optimized conditions, the reactions were performed using a 10 mM $FeCl_3{\cdot}6\ H_2O$ (17.8 μmol, 2 mol %) solution in acetonitrile pressurized with O_2 in a photoreactor, and the product mixture was analyzed by GC−MS. Together with acetone, other oxidation products were identified, namely—in decreasing proportions—acetic acid, acetaldehyde, propionaldehyde, isopropanol, and 1-propanol (Figure S2). To investigate photoactive species, a thorough catalytic screening involving different iron sources and metal chlorides was carried out. When a list of available transition metal chlorides was considered, only copper(II) chloride performed comparably with iron(III) chloride (Figure 1a). This is consistent with previous works discussing both $FeCl_3$ and $CuCl_2{\cdot}2H_2O$ in light-driven oxidation of alkanes.[13,14] Propane was successfully photooxidized when $FeCl_3$ was replaced by $FeBr_3$, but to a much lower extent (Figure 1b). The rate for acetone production was respectively about and more than five times lower for $Fe(NO_3)_3{\cdot}9H_2O$ and $Fe_2(SO_4)_3{\cdot}xH_2O$ compared with $FeCl_3$ (Figure 1c), stressing again the essential role of the halide. Next, the oxidation state of iron was considered. In a photoinduced scenario, iron(III) might be the precursor of an active species generated under irradiation. Iron(III) is known to undergo photoreduction to iron(II), also in natural environments.[15,16] To test whether iron(II) was the real active species taking part in the process, $FeCl_2$ was used as a catalyst. The ferrous salt did not outperform $FeCl_3{\cdot}6H_2O$. Nevertheless, the acetone quantified was not negligible (Figure 1d), once iron(II) is predictably oxidized to iron(III) under aerobic conditions.

In our best result, propane underwent 100% conversion with 67% selectivity in acetone in 4 h (Figure 2b,c). After this time, the reaction reached a plateau, and no further improvements in acetone selectivity were achieved. After 8 h, no further conversion could occur since a complete drop of pressure was observed in the reactor. By contrast, the quantification of products in the liquid phase revealed a decrease in conversion for longer times (Figure S3). This can be ascribed to the overoxidation of products to carbon dioxide, which was indeed detected by GC−MS in the gas phase. Propane conversion to acetone increased linearly when iron concentration was varied between 0.05 and 10 mM and slightly decreased with higher amounts of the iron salt (Figure 2d). The turnover number (TON)—calculated as the ratio of moles of acetone to moles of $FeCl_3$—reached a high of over 600 when 0.05 mM $FeCl_3{\cdot}6H_2O$ (0.01 mol %) was used. Interestingly, a very similar trend was previously reported in works on the photooxidation of hydrocarbons catalyzed by homogeneous $FeCl_3$ as well as heterogeneous TiO_2.[7,17] This profile was interpreted as evidence for the critical role of light. Indeed, for small concentrations of the photoactive species, the absorbance is defined by the Lambert−Beer equation: the higher the concentration, the higher the number of photons absorbed. Thus, yield is expected to increase with absorbance. Nevertheless, at very high concentrations, the absorption of photons is saturated (see Supporting Information for a detailed discussion).

The trend in acetone yield reproduced the UV−vis profile of $FeCl_3$ in acetonitrile when the reaction was carried out under different irradiation wavelengths, as shown in Figure S1. The acetone yield decreased at longer wavelengths. Interestingly, $FeCl_3$ in acetonitrile exhibits two major peaks at 313 and 360 nm. Optical transitions of iron hydroxides and chlorides in aqueous solutions were previously thoroughly investigated, and it was concluded that broad transitions between 270 and 400 nm are attributed to charge transfer states.[18,19] The comparison between the absorption spectra of $FeCl_3{\cdot}6H_2O$ in water and acetonitrile, as well as in other solvents, is reported in Figure S4a−e.

Mechanistic Studies. First, the performance of photooxidation was probed in the presence of additives as quenchers (Figure 3a). In a semiconductor-like scenario, the excitation by light is followed by charge separation, and reactivity is highly affected by the presence of sacrificial reagents. In particular, a photooxidation reaction is supposed to be enhanced by sacrificial electron acceptors. The addition of potassium persulfate ($K_2S_2O_8$) resulted in a decrease in the rate of the reaction. The same was observed when glycerin was added as a sacrificial electron donor. In any case, the sacrificial reagents

https://doi.org/10.1021/acscatal.3c02092
ACS Catal. 2023, 13, 8662−8669

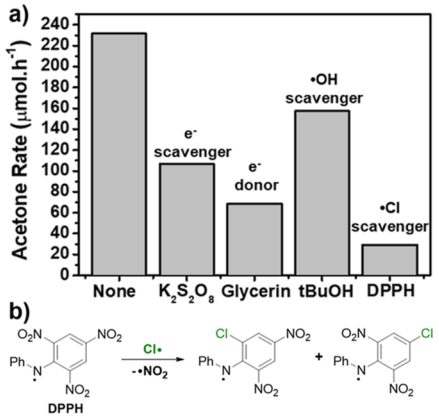

Figure 3. (a) Quenching experiments to probe aerobic $FeCl_3$-catalyzed propane photooxidation. Conditions: 2 mL CH_3CN, $FeCl_3 \cdot 6H_2O$ (17.8 μmol, 1.6 mol %), 3.4 bar O_2, 2.8 bar propane (1.1 mmol), 410 nm (100 W), 1 h, r.t., $K_2S_2O_8$ (100 μmol), Glycerin (100 μmol), tBuOH (100 μmol), DPPH (20 μmol); (b) Chlorine radical trapping by substitution reaction on DPPH.

did not improve acetone production whatsoever. Despite a mixture of $FeCl_3$ and H_2O_2 did not photooxidize propane at comparable rates as under aerobic conditions (Table 1, entry 4), a photo-assisted Fenton-like scenario was still under debate. Therefore, the reaction was repeated introducing tert-butanol (tBuOH), a standard quencher of hydroxyl radicals.[20] No difference was observed from optimized conditions, indicating that hydroxyl radicals are not relevant species. Instead, synthesized acetone dramatically decreased upon the addition of 2,2-diphenyl-1-picrylhydrazyl (DPPH), a well-known chlorine radical trap.[21] Moreover, two additional peaks were detected in the GC−MS chromatograms after the reaction, which were assigned to the different isomers resulting from the radical substitution reaction to DPPH (Figures 3b, S6). The result strongly indicates the generation of chlorine radicals in solution.

Radicals in C−H activation usually occur together with HAT. Thus, chlorine radicals might abstract hydrogen atoms from propane, yielding alkyl radicals. If the C−H homolytic cleavage occurs before or as part of the rate-determining step, the reaction is expected to slow down by isotopic substitution due to a primary kinetic isotope effect (KIE). To test this hypothesis, cyclohexane was used as a model substrate under the same aerobic conditions applied to propane photooxidation. As shown in Figure S7a, a small KIE of 1.67 was found. This is consistent with the result reported by Shul'pin et al.[7] Conversely, KIEs higher than 10 are typical of C−H activation from biomimetic iron(IV)-oxo species.[22,23] KIEs below 4 are consistent with hydrogen atom abstraction on hydrocarbons by photogenerated chlorine radicals.[24]

In order to probe the formation of alkyl radical intermediates, adamantane was used as a model hydrocarbon. The higher stability of tertiary radicals should favor the functionalization of adamantane at carbon 1. Adamantan-1-ol, adamantan-2-ol, adamantanone, and 1-chloroadamantane were detected after 1 h of irradiation (Figure S7b,c). The relative ratio of 1-substituted to 2-substituted products, normalized per the number of hydrogen atoms, was 1.14. The detection of the tertiary 1-chloroadamantane supported the presence of chlorine radicals and chlorination via the radical termination pathway. Such a low value of 3°/2° substitution is typical of a radical-based rather than a Fe(IV) = O-based mechanism. Typical normalized 3°/2° selectivity ratios for HO· and tBuO·-based radical chain autoxidation were reported to be 2 and 10, respectively, while ratios higher than 15 are expected for biomimetic oxo-metal-carbon interaction.[25] In situ generation of chlorine radicals can be easily explained by photolysis of the Fe−Cl bond ($Fe^{III}-Cl + h\nu \rightarrow Fe^{II} + Cl\cdot$). Photolysis of Fe^{III}−OH and Fe^{III}−Cl bonds was observed previously and thoroughly characterized via transient spectroscopy in aqueous solution when irradiated under ultraviolet light.[26] Detailed UV−vis experiments indicated the conversion of Fe^{III} into Fe^{II} species (Figure S8a−c), suggesting the formation of Fe(II) from Fe^{III}−Cl photolysis.

Further characterization was carried out to better identify the active catalytic species. Mössbauer spectroscopy did not detect any iron (IV) species in solution, suggesting that biomimicking iron-oxo species are not relevant to the mechanism in this work (Figure S9).

Additionally, electrospray ionization mass spectrometry (ESI-MS) was performed to detect iron complexes in acetonitrile. When operated in positive mode, the mass spectrum exhibited a peak at 207.9255 m/z, which is consistent with the tetrahedral complex $[Fe(CH_3CN)_2Cl_2]^+$. The isotopic distribution matched very well the theoretical prediction (Figure S10a). In order to confirm the attribution, a MS/MS spectrum was recorded. Daughter ions at 166.8985, 131.9295, and 125.8716 m/z, corresponding to the loss of fragments $(FeCH_3CN)^+$, $(FeCH_3CNCl)^+$, and $[(Fe(CH_3CN)_2]^+$ (Figure S10b) were observed. A further peak at 172.9574 m/z might be attributed to the iron(II) counterpart $[Fe(CH_3CN)_2Cl]^+$ (Figure S10c). When the instrument was operated in negative mode, a sharp peak at 197.8083 m/z appeared. This was attributed to the well-known tetrahedral complex $FeCl_4^-$. Two peaks at 162.8397 and 160.847 m/z, corresponding respectively to the loss of ^{35}Cl and ^{37}Cl, were detected in the corresponding MS/MS spectrum (Figure S10d).

Dai et al. observed the photocatalytic activity of a mixture of $FeCl_3$/HCl in C−H activation and proposed that $FeCl_4^-$ can generate chlorine radicals when irradiated by violet light through a LMCT excitation.[8] Tetrahedral species of iron (III), such as $[Fe(CH_3CN)_2Cl_2]^+$, which appeared to be the most abundant, also can undergo the photolysis of the Fe−Cl bond, generating chlorine radicals. Our data suggest that acetonitrile might be non-innocent. Indeed, the absorbance spectrum of $FeCl_3$ is highly dependent on the solvent (Figure S4d). The presence of solvent molecules in the first coordination sphere of Fe complexes is expected to dramatically affect the electronic states and, consequently, optical properties. LMCT or MLCT transitions provided by the interaction between acetonitrile and the metal center might actually cause the outstanding observed photoactivity. To demonstrate that the absorbance does not originate from $FeCl_4^-$ itself, we also recorded UV−vis spectra of 1-butyl-3-methylimidazolium tetrachloroferrate ([bmim][$FeCl_4$]) in acetonitrile and different solvents (Figure S5). The spectrum in acetonitrile presented the same features of a $FeCl_3$ solution, while a great variability was observed again in other solvents.

Our DFT calculations also pointed to the formation of relevant iron complexes. The ground state energy of the PBEh-3c optimized $FeCl_3$, its dimeric species Fe_2Cl_6, and the $[FeCl_4]^-[FeCl_2(CH_3CN)_4]^+$ and $[FeCl_4]^-[FeCl_2(CH_3CN)_2]^+$ salts[27] (Figure S10e,f) were compared, including the solvent effects of MeCN, using the CPCM model. To compare the

https://doi.org/10.1021/acscatal.3c02092
ACS Catal. 2023, 13, 8662−8669

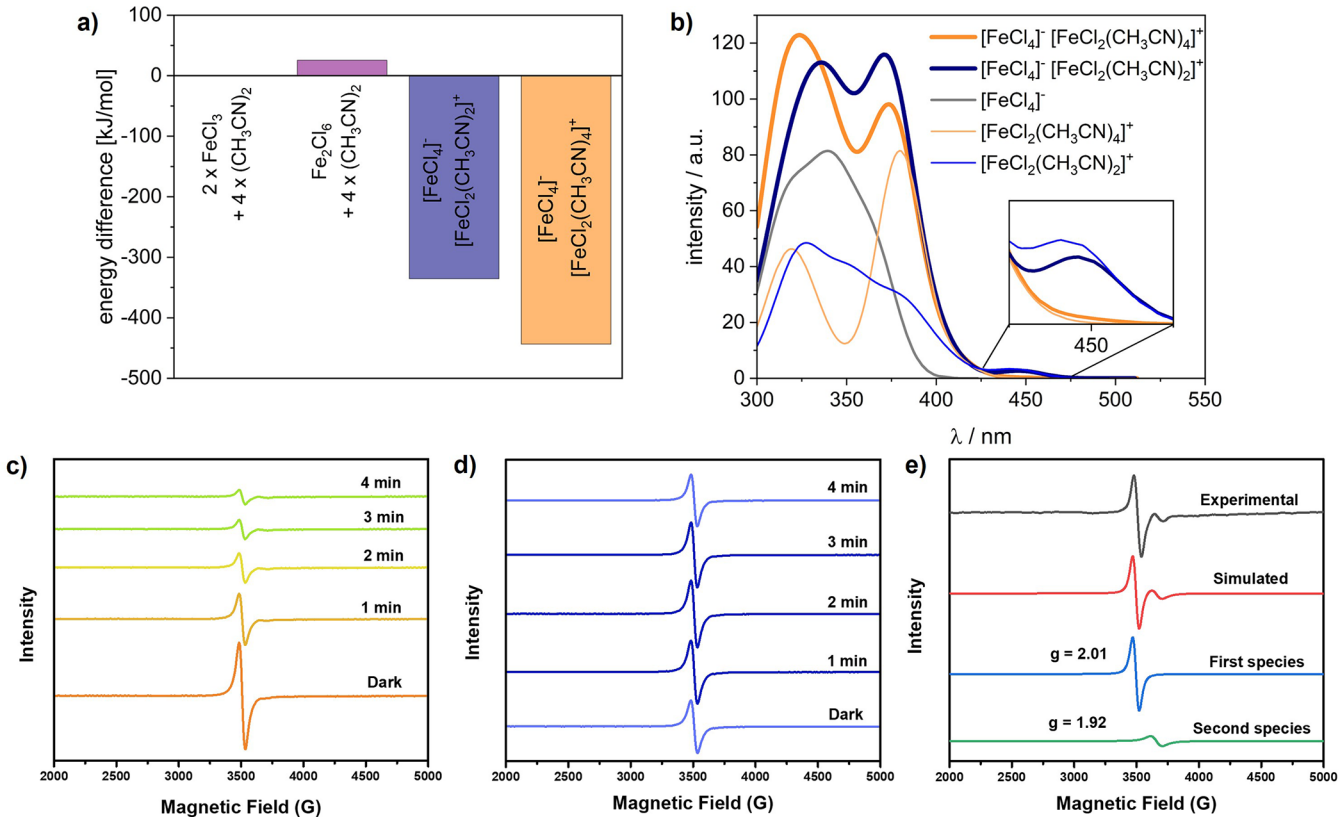

Figure 4. (a) Energy difference between the single point energy of the PBEh-3c geometry optimized species related to 2 × $FeCl_3$ + 4 × MeCN. (b) TD-DFT simulated UV−vis spectra of $[FeCl_4]^-$ $[FeCl_2(CH_3CN)_4]^+$ and $[FeCl_4]^-$ $[FeCl_2(CH_3CN)_2]^+$ and its ionic components in acetonitrile (CPCM); (c) EPR irradiated spectra over time of 1 mM $FeCl_3$ acetonitrile solution under argon and (d) oxygen atmosphere; (e) experimental and simulated spectra of the argon system after the 4 min of irradiation.

ground-state energy of the same number of atoms, also the energy of gas phase MeCN molecules was calculated and added (Figure 4a). Especially both salts show a dramatic increase in terms of stability. Based on this evidence, the UV−vis transitions of the two in total neutral species and their ionic components were calculated (Figure 4b). The calculated spectra of both salts fit the experimental spectrum and reproduce the two bands at 360 and 313 nm. For $[FeCl_4]^-[FeCl_2(CH_3CN)_4]^+$, the low energy signal at around 375 nm in the calculated spectra can be attributed to an LMCT process from the MeCN ligand to the Fe center of the cationic species $[FeCl_2(CH_3CN)_4]^+$, whereas the higher energy signal at around 325 nm stems from an LMCT process at the $[FeCl_4]^-$. This also becomes visible when the calculated spectra of both separated ions are compared since the cation has a larger impact on the low energy band and the anion on the high energy band. For $[FeCl_4]^-[FeCl_2(CH_3CN)_2]^+$, an additional weak band at 450 nm appears, reproducing the shallow sloping of the 360 nm band in the experiment.

Although some authors proposed $FeCl_4^-$ as photoactive species,[28,29] we claim that other iron complexes should be considered. To test this hypothesis, results from catalytic tests performed in excess sulfuric acid and hydrochloric acid were compared. We observed 77% decrease in activity when H_2SO_4 was replaced with HCl under the same conditions (Figure S11). Similarly, very poor catalytic activity was obtained by replacing $FeCl_3$ with a tetrachloroferrate salt (Figure S12). This finding indicates that the photoactivity should not be attributed to $FeCl_4^-$ ions, given that the equilibrium shifts to the formation of this species when HCl is added to the solution (a larger concentration of Cl^-).

Figure 4c,d shows the electroparamagnetic resonance (EPR) measurements of the $FeCl_3$ acetonitrile solution in argon and oxygen atmospheres, respectively. Before switching on the light, a sharp transition line at g ∼ 2.01 was detected. This is characteristic of isotropic non-ferromagnetic Fe^{III}, i.e., these species are not aggregate or in a cluster shape. During the irradiation of the argon system, the signal decreased as a function of time, losing about 90% of the initial area after 4 min. This loss was not reversible and can be associated with the conversion of Fe^{III} to Fe^{II} through the production of the chlorine radical (Fe^{III}−Cl + hv → Fe^{II} + Cl·). Furthermore, a paramagnetic signal (g = 1.91) was also detected when the main Fe^{III} transition line dropped, and this was stable under 395 nm irradiation over time (Figure 4e). The same signal was also observed when the solution was diluted ten times (0.1 mM), which means it is not a transient species. Based on the light stability, we propose that this hidden transition line comes from $FeCl_4^-$. To investigate this hypothesis, an EPR spectrum of [bmim][$FeCl_4$] was recorded at room temperature in acetonitrile. The signal at g = 1.91 was clearly visible, along with two more at g = 4.31 and g = 2.01 (Figure S13). Usually transition lines around g ∼ 4.3 are associated with Fe^{3+} in tetrahedral coordination, while those close to g ∼ 2.0 are assigned to octahedral chemical environments.[30−32] The existence of more than one signal suggests a mixture of complexes in our system, which is consistent with the co-presence of $FeCl_4^-$ and other tetrahedral Fe species like those identified by ESI-MS and DFT calculations.

https://doi.org/10.1021/acscatal.3c02092
ACS Catal. 2023, 13, 8662−8669

The spin trapping tests under argon yielded a spin adduct with six transition lines, with the hyperfine constants of 13.5 and 10.0 G (Figure S14a). Normally, this type of spectrum is due to the DMPO degradation, which is reasonable, since the chlorine adduct is not stable.[33,34] Interestingly, no signal was observed when this same measurement was performed in O_2. However, when cyclohexane was added, a six-line signal was detected with the hyperfine values of 13.1 and 8.5 G (Figure S14b), which are related to organic peroxide.[35] In Figure S14c, it is easy to distinguish the features of these simulated spin adducts and see that with oxygen and in the absence of cyclohexane, no radical was detected.

Mechanism Proposal. Data collected in this work strongly suggest that the direct photocatalytic conversion of propane in acetone presented is governed by a radical-based mechanism. In particular, this system fits in very well with the mechanism proposed by Shul'pin et al.[7] The catalytic cycle is initiated by photolysis of the Fe−Cl bond. Then, a typical radical chain follows (Scheme 1). In general, the reaction is initiated by a

Scheme 1. Mechanism Proposal of $FeCl_3$-Catalyzed Propane Photooxidation

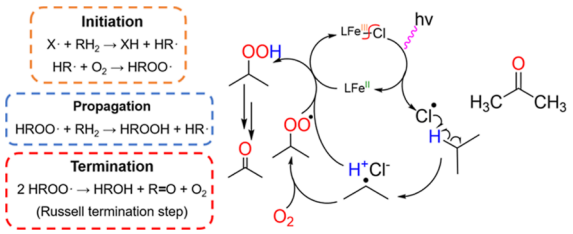

suitable hydrogen atom-abstracting species (in most cases, a free radical), which generates an alkyl radical. Molecular dioxygen swiftly combines with it, yielding an alkyl peroxyl radical. This species can subsequently abstract hydrogen atoms from other alkane molecules, forming alkyl hydroperoxides and propagating the reaction. Two main termination steps can be considered. The alkyl peroxyl radical can either dimerize and decompose to an alcohol, a ketone, and dioxygen or receive an electron from a donating species and undergo protonation to yield an alkyl hydroperoxide.[36] The former pathway is also known as the Russell termination step, named after Glen A. Russell, who first proposed the decomposition of a dimer of alkyl peroxyl radicals via reverse cycloaddition.[37]

A Russell termination step is characterized by an alcohol/ketone ratio not higher than one (A/K ≤ 1). Indeed, even if alcohols and ketones are produced in a 1:1 ratio, alcohols can be further oxidized due to the presence of oxidant species, such as Cl radical. Table S2 summarizes the A/K ratios observed in the photooxidation of different hydrocarbons. In all cases, A/K was below 1, which is consistent with a Russell termination step. The very low ratio obtained for propane can be explained with a very fast oxidation of isopropanol to acetone under aerobic conditions. 1-propanol and 2-propanol were detected in very low amounts in catalytic tests (Figure 2c). Moreover, 2-propanol (isopropanol) oxidation under the same catalytic conditions was investigated. Isopropanol was oxidized at a slightly faster rate than propane at the same molar amount (Figure S15). This result supports the hypothesis of a Russell termination step and is consistent with the low A/K ratio observed for propane. As soon as isopropanol is generated in this step, it is swiftly converted to acetone. In order to close the catalytic cycle, the active Fe^{III} active species must be regenerated. The most likely species able to promote the Fe^{II} oxidation back to Fe^{III} are the propyl peroxyl radicals. In turn, they get reduced and protonated to alkyl hydroperoxides, that might subsequently decompose to ketones (Scheme 1). In the proposed mechanism, O_2 is also responsible for the regeneration of Fe^{III} species, as demonstrated by the EPR data (Figure 4).

CONCLUSIONS

A facile method for aerobic propane photooxidation into acetone was successfully developed, employing as a homogeneous photocatalyst a simple $FeCl_3$ solution in acetonitrile. In the best outcome, 100% conversion of propane with 69% selectivity in acetone was achieved after 4 h of irradiation under violet light. A thorough catalytic screening confirmed that both iron(III) and chloride anions are needed in order to promote the catalysis. Multiple mechanistic studies support a radical-based mechanism involving the generation of chlorine radicals resulting from Fe−Cl photolysis and subsequent HAT. KIE (1.67), the 3°/2° functionalization ratio of adamantane (1.14), and the alcohol-to-ketone (A/K) synthesis ratio (≤1) were consistent with a radical process rather than a biomimicking, Fe(IV)-based one. The coordinating ability of the solvent may play a major role to favor the Fe−Cl bond cleavage upon irradiation or to stabilize the photoactive species. ESI-MS combined with Mössbauer spectroscopy and DFT calculations identified $[Fe(CH_3CN)_2Cl_2]^+$ as the likely active species. Our mechanism investigation shed light on this interesting reaction, demonstrating that $FeCl_4^-$ species were not the most active species for C−H oxidation.

Overall, this work seems to confirm the reputation of iron-based C−H activation as a "holy grail" of modern chemistry. We strongly believe that the synthesis of valuable chemical feedstocks, including acetone and acetic acid, under very mild conditions holds promise for the development of sustainable industrial conversions of hydrocarbons.

ASSOCIATED CONTENT

Supporting Information

The Supporting Information is available free of charge at https://pubs.acs.org/doi/10.1021/acscatal.3c02092.

Experimental procedures, details of computational studies, UV−vis spectrum, GC−MS chromatogram of the product mixture of aerobic propane photooxidation, kinetics of propane photooxidation, normalized UV−vis spectra, and experimental data (PDF)

AUTHOR INFORMATION

Corresponding Author

Ivo F. Teixeira − *Department of Colloid Chemistry, Max Planck Institute of Colloids and Interfaces, Potsdam 14476, Germany; Department of Chemistry, Federal University of São Carlos, 13565-905 São Paulo, Brazil;* orcid.org/0000-0002-4356-061X; Email: ivo@ufscar.br

Authors

Andrea Rogolino − *Galilean School of Higher Education, University of Padova, Padova 35131, Italy; Department of Colloid Chemistry, Max Planck Institute of Colloids and Interfaces, Potsdam 14476, Germany;* orcid.org/0000-0001-7632-0658

https://doi.org/10.1021/acscatal.3c02092
ACS Catal. 2023, 13, 8662−8669

José B. G. Filho − *Department of Chemistry, ICEx, Federal University of Minas Gerais, Belo Horizonte 31270-901 Minas Gerais, Brazil;* orcid.org/0000-0003-1641-6476
Lorena Fritsch − *AK Bauer, University of Paderborn, Paderborn D-33098, Germany*
José D. Ardisson − *Applied Physics Lab, CDTN, Campus da Universidade Federal de Avenida Presidente Antônio Carlos, Belo Horizonte, Minas Gerais 31270-901, Brazil*
Marcos A. R. da Silva − *Department of Chemistry, Federal University of São Carlos, 13565-905 São Paulo, Brazil*
Gabriel Ali Atta Diab − *Department of Chemistry, Federal University of São Carlos, 13565-905 São Paulo, Brazil;* orcid.org/0000-0002-5423-7658
Ingrid Fernandes Silva − *Department of Colloid Chemistry, Max Planck Institute of Colloids and Interfaces, Potsdam 14476, Germany*
Carlos André Ferreira Moraes − *Department of Chemistry, Federal University of São Carlos, 13565-905 São Paulo, Brazil*
Moacir Rossi Forim − *Department of Chemistry, Federal University of São Carlos, 13565-905 São Paulo, Brazil;* orcid.org/0000-0001-8798-2921
Matthias Bauer − *AK Bauer, University of Paderborn, Paderborn D-33098, Germany;* orcid.org/0000-0002-9294-6076
Thomas D. Kühne − *Dynamics of Condensed Matter and Center for Sustainable System Design, Chair of Theoretical Chemistry, University of Paderborn, Paderborn D-33098, Germany*
Markus Antonietti − *Department of Colloid Chemistry, Max Planck Institute of Colloids and Interfaces, Potsdam 14476, Germany;* orcid.org/0000-0002-8395-7558

Complete contact information is available at: https://pubs.acs.org/10.1021/acscatal.3c02092

Author Contributions

The manuscript was written through contributions of all authors. AR and IFT conceived and coordinated all stages of this research in collaboration with MA. IFT, AR, MARS, and GAAD undertook the catalytic tests. LF, MB, and TDK conducted the computational studies. JBGF conducted the EPR experiments. CAFM and MRF performed ESI-MS analysis. JDA acquired and fitted the Mössbauer spectra.

Funding

Open access funded by Max Planck Society.

Notes

The authors declare no competing financial interest.

■ ACKNOWLEDGMENTS

This research was financially supported by the Brazilian funding agencies CAPES, CNPq (423196/2018-9 and 403064/2021-0), FAPESP (2020/14741-6, 2021/14006-7, 2021/13271-9, and 2021/11162-8) and the Max Planck Society. I.F.T. thanks the Alexander von Humboldt Foundation for his postdoctoral fellowship. M.B. kindly acknowledges financial support from the German BMBF in the frame of projects Syn-XAS (FKZ 05K18PPA) and FocusPP64 (FKZ05K19PP1). L.F. thanks the Fonds der Chemischen Industrie for funding via a Kekulé grant.

■ REFERENCES

(1) Kerr, J. Bond dissociation energies by kinetic methods. *Chem. Rev.* **1966**, *66*, 465−500.
(2) Zakoshansky, V. The cumene process for phenol-acetone production. *Pet. Chem.* **2007**, *47*, 273−284.
(3) Schuchardt, U.; Carvalho, W. A.; Spinacé, E. V. Why is it interesting to study cyclohexane oxidation? *Synlett* **1993**, *1993*, 713−718.
(4) Cook, G. K.; Mayer, J. M. CH bond activation by metal oxo species: Oxidation of cyclohexane by chromyl chloride. *J. Am. Chem. Soc.* **1994**, *116*, 1855−1868.
(5) Wang, K.; Mayer, J. M. Oxidation of Hydrocarbons by $[(phen)_2Mn(\mu\text{-}O)_2Mn(phen)_2]^{3+}$ via Hydrogen Atom Abstraction. *J. Am. Chem. Soc.* **1997**, *119*, 1470−1471.
(6) Chaudhuri, P.; Hess, M.; Flörke, U.; Wieghardt, K. From structural models of galactose oxidase to homogeneous catalysis: efficient aerobic oxidation of alcohols. *Angew. Chem., Int. Ed.* **1998**, *37*, 2217−2220.
(7) Shul'pin, G. B.; Nizova, G. V.; Kozlov, Y. N. Photochemical aerobic oxidation of alkanes promoted by iron complexes. *New J. Chem.* **1996**, *20*, 1243−1256.
(8) Dai, Z.-Y.; Zhang, S.-Q.; Hong, X.; Wang, P.-S.; Gong, L.-Z. A practical $FeCl_3$/HCl photocatalyst for versatile aliphatic C−H functionalization. *Chem Catal.* **2022**, *2*, 1211−1222.
(9) Oh, S.; Stache, E. E. Chemical Upcycling of Commercial Polystyrene via Catalyst-Controlled Photooxidation. *J. Am. Chem. Soc.* **2022**, *144*, 5745−5749.
(10) Kang, Y. C.; Treacy, S. M.; Rovis, T. Iron-catalyzed photoinduced LMCT: A 1° C−H abstraction enables skeletal rearrangements and C (sp3)−H alkylation. *ACS Catal.* **2021**, *11*, 7442−7449.
(11) Fenton, H. J. H. LXXIII.—Oxidation of tartaric acid in presence of iron. *J. Chem. Soc., Trans.* **1894**, *65*, 899−910.
(12) Haber, F.; Weiss, J.; Pope, W. J. The catalytic decomposition of hydrogen peroxide by iron salts. *Proc. R. Soc. London, Ser. A* **1934**, *147*, 332−351.
(13) Takaki, K.; Yamamoto, J.; Matsushita, Y.; Morii, H.; Shishido, T.; Takehira, K. Oxidation of alkanes with dioxygen induced by visible light and Cu (II) and Fe (III) chlorides. *Bull. Chem. Soc. Jpn.* **2003**, *76*, 393−398.
(14) Takaki, K.; Yamamoto, J.; Komeyama, K.; Kawabata, T.; Takehira, K. Photocatalytic oxidation of alkanes with dioxygen by visible light and copper (II) and iron (III) chlorides: preference oxidation of alkanes over alcohols and ketones. *Bull. Chem. Soc. Jpn.* **2004**, *77*, 2251−2255.
(15) Pehkonen, S. O.; Siefert, R.; Erel, Y.; Webb, S.; Hoffmann, M. R. Photoreduction of iron oxyhydroxides in the presence of important atmospheric organic compounds. *Environ. Sci. Technol.* **1993**, *27*, 2056−2062.
(16) McKnight, D.; Kimball, B.; Bencala, K. Iron photoreduction and oxidation in an acidic mountain stream. *Science* **1988**, *240*, 637−640.
(17) Mu, W.; Herrmann, J.-M.; Pichat, P. Room temperature photocatalytic oxidation of liquid cyclohexane into cyclohexanone over neat and modified TiO_2. *Catal. Lett.* **1989**, *3*, 73−84.
(18) Nadtochenko, V. A.; Kiwi, J. Photolysis of $FeOH^{2+}$ and $FeCl^{2+}$ in aqueous solution. Photodissociation kinetics and quantum yields. *Inorg. Chem.* **1998**, *37*, 5233−5238.
(19) Rabinowitch, E. Electron Transfer Spectra and Their Photochemical Effects. *Rev. Mod. Phys.* **1942**, *14*, 112−131.
(20) Cederbaum, A. I.; Qureshi, A.; Cohen, G. Production of formaldehyde and acetone by hydroxyl-radical generating systems during the metabolism of tertiary butyl alcohol. *Biochem. Pharmacol.* **1983**, *32*, 3517−3524.
(21) Seto, A.; Ochi, Y.; Gotoh, H.; Sakakibara, K.; Hatazawa, S.; Seki, K.; Saito, N.; Mishima, Y. Trapping chlorine radicals via substituting nitro radicals in the gas phase. *Anal. Methods* **2016**, *8*, 25−28.

(22) Costas, M.; Chen, K.; Que, L. Biomimetic nonheme iron catalysts for alkane hydroxylation. *Coord. Chem. Rev.* **2000**, *200*−*202*, 517−544.
(23) Company, A.; Gómez, L.; Güell, M.; Ribas, X.; Luis, J. M.; Que, L.; Costas, M. Alkane hydroxylation by a nonheme iron catalyst that challenges the heme paradigm for oxygenase action. *J. Am. Chem. Soc.* **2007**, *129*, 15766−15767.
(24) Tschuikow-Roux, E.; Niedzielski, J.; Faraji, F. Competitive photochlorination and kinetic isotope effects for hydrogen/deuterium abstraction from the methyl group in C_2H_6, C_2D_6, CH_3CHCl_2, CD_3CHCl_2, CH_3CCl_3, and CD_3CCl_3. *Can. J. Chem.* **1985**, *63*, 1093−1099.
(25) Talsi, E. P.; Bryliakov, K. P. Chemo- and stereoselective CH oxidations and epoxidations/cis-dihydroxylations with H_2O_2, catalyzed by non-heme iron and manganese complexes. *Coord. Chem. Rev.* **2012**, *256*, 1418−1434.
(26) Kiwi, J.; Pulgarin, C.; Peringer, P.; Grätzel, M. Beneficial effects of homogeneous photo-Fenton pretreatment upon the biodegradation of anthraquinone sulfonate in waste water treatment. *Appl. Catal., B* **1993**, *3*, 85−99.
(27) Gao, Y.; Guery, J.; Jacoboni, C. $FeCl_3$ behavior in acetonitrile: structures of $[FeCl_2\ (CH_3CN)_4]$ $[FeCl_4]$ and $[AlCl(CH_3CN)_5]$ $[FeCl_4]_2$. CH_3CN. *Acta Crystallogr., Sect. C: Cryst. Struct. Commun.* **1993**, *49*, 147−151.
(28) Li, S.; Zhu, B.; Lee, R.; Qiao, B.; Jiang, Z. Visible light-induced selective aerobic oxidative transposition of vinyl halides using a tetrahalogenoferrate(iii) complex catalyst. *Org. Chem. Front.* **2018**, *5*, 380−385.
(29) Fahy, K. M.; Liu, A. C.; Barnard, K. R.; Bright, V. R.; Enright, R. J.; Hoggard, P. E. Photooxidation of Cyclohexane by Visible and Near-UV Light Catalyzed by Tetraethylammonium Tetrachloroferrate. *Catalysts* **2018**, *8*, 403.
(30) Pathak, N.; Gupta, S. K.; Sanyal, K.; Kumar, M.; Kadam, R. M.; Natarajan, V. Photoluminescence and EPR studies on Fe^{3+} doped $ZnAl_2O_4$: an evidence for local site swapping of Fe^{3+} and formation of inverse and normal phase. *Dalton Trans.* **2014**, *43*, 9313−9323.
(31) Kucherov, A. V.; Shelef, M. Quantitative Determination of Isolated Fe^{3+} Cations in FeHZSM-5 Catalysts by ESR. *J. Catal.* **2000**, *195*, 106−112.
(32) Aboukaïs, A.; Zhilinskaya, E. A.; Filimonov, I. N.; Nesterenko, N. S.; Timoshin, S. E.; Ivanova, I. I. EPR investigation, before and after adsorption of naphtalene, of mordenite containing Fe^{3+} and Cr^{5+} ions as impurities. *Catal. Lett.* **2006**, *111*, 97−102.
(33) Bernofsky, C.; Bandara, B. M. R.; Hinojosa, O. Electron spin resonance studies of the reaction of hypochlorite with 5,5-dimethyl-1-pyrroline-N-oxide. *Free Radicals Biol. Med.* **1990**, *8*, 231−239.
(34) Schaich, K. M.; Borg, D. C. Fenton reactions in lipid phases. *Lipids* **1988**, *23*, 570−579.
(35) Davies, M. J.; Slater, T. F. Studies on the photolytic breakdown of hydroperoxides and peroxidized fatty acids by using electron spin resonance spectroscopy. Spin trapping of alkoxyl and peroxyl radicals in organic solvents. *Biochem. J.* **1986**, *240*, 789−795.
(36) Simic, M. G. Free radical mechanisms in autoxidation processes. *J. Chem. Educ.* **1981**, *58*, 125.
(37) Russell, G. A. Deuterium-isotope effects in the autoxidation of aralkyl hydrocarbons. mechanism of the interaction of peroxy radicals1. *J. Am. Chem. Soc.* **1957**, *79*, 3871−3877.

https://doi.org/10.1021/acscatal.3c02092
ACS Catal. 2023, 13, 8662−8669